Porphyrin–fullerene linked systems as artificial photosynthetic mimics

Hiroshi Imahori*

Department of Molecular Engineering, Graduate School of Engineering, Kyoto University, PRESTO, JAPAN Science and Technology Agency (JST), Katsura, Nishikyo-ku, Kyoto 615-8510, Japan and Fukui Institute for Fundamental Chemistry, Kyoto University, 34-4, Takano-Nishihiraki-cho, Sakyo-ku, Kyoto 606-8103, Japan. E-mail: imahori@scl.kyoto-u.ac.jp; Fax: +81-75-383-2571

We have prepared a variety of porphyrin–fullerene linked systems to mimic photoinduced energy and electron transfer (ET) processes in photosynthesis. Photodynamical studies on porphyrin and analogs–fullerene linked systems have revealed the acceleration of photoinduced electron transfer and charge-shift and the deceleration of charge recombination, which is reasonably explained by the small reorganization energies of electron transfer in fullerenes. In this context, we have proposed two strategies, photo-induced single-step and multi-step electron transfers, for prolonging the lifetime of a charge-separated state in donor–acceptor linked systems. The single-step ET strategy allowed a zinc chlorin–fullerene linked dyad to extend the lifetime up to 120 seconds in frozen PhCN at 123 K, which is the longest value of charge separation ever reported for donor–acceptor linked systems. Unfortunately, however, the quantum yield of formation of the charge-separated state was as low as 12%, probably due to the decay of the precursor exciplex state to the ground state rather than to the favorable complete charge-separated state. In contrast, the multi-step ET strategy has been successfully applied to porphyrin–fullerene linked triads, tetrads, and a pentad. In particular, a ferrocene–porphyrin trimer–fullerene pentad revealed formation of a long-lived charge-separated state (0.53 s in frozen DMF at 163 K) with an extremely high quantum yield (83%), which is comparable to natural bacterial reaction centers. These results not only provide valuable information for a better understanding of photoinduced energy and electron transfer processes in photosynthesis, but also open the door for the development of photo-initiated molecular devices and machines.

1 Introduction

Recently, researchers have paid much attention to artificial photosynthesis in terms of nanoscience and nanotechnology as well as energy and environmental problems.[1] Artificial photosynthesis involves the mimicry of photosynthetic processes and the application of basic principles in photosynthesis to energy conversion systems and molecular devices. For instance, photo-active molecular devices and machines, which act as sensors, memories, and switches at a molecular level, have been extensively investigated aiming for the goal of replacing conventional electronic devices by molecular devices.[1] Practical challenges in artificial photosynthesis lie in the development of organic solar cells, photocatalysts, and others. Thus, a variety of researchers, including chemists, physicists, materials scientists, and biologists, have been involved in artificial photosynthesis.[1] The photosynthetic system is regarded as the most elaborate nano-scale biological machine in nature.[2,3] It converts solar energy eventually into chemical energy, which is prerequisite for living organisms on the earth. The key process of photosynthesis is a cascade of photoinduced energy transfer (EN) and subsequent electron transfer (ET) between donors and acceptors embedded in the antenna complexes and reaction centers. For example, in purple photosynthetic bacteria, visible light is harvested by the antenna complexes, including bacteriochlorophylls (Bchl) and carotenoid polyenes, and the collected energy is funneled into the bacteriochlorophyll dimer (special pair) in the reaction center, where multi-step electron transfers take place.[2,3] Namely, within ~3 ps, an ET occurs from the singlet excited state of special pair ^{1}(Bchl)$_2$*, which lies about 1.4 eV above the ground state, to the bacteriopheophytin (Bphe) molecule located ~9 Å (= R_{ee}: edge-to-edge distance) *via* a two-step sequential mechan-

Hiroshi Imahori was born in Kyoto, Japan in 1961. He completed his doctorate with Professor Kazuhiro Maruyama at Kyoto University on the electron-transfer photochemistry of quinones. From 1990–1992 he was a post-doctoral fellow in Professor Tan Inoue's group at the Salk Institute for Biological Studies at La Jolla, USA, working on the development of in vitro selection systems of catalytic RNA (ribozyme). In 1992 he joined the group of Professor Yoshiteru Sakata at Osaka University, as an Assistant Professor. In 1999 he moved to the group of Professor Shunichi Fukuzumi at the Graduate School of Engineering, Osaka University, as an Associate Professor. Since 2002 he has been Professor of Chemistry, Graduate School of Engineering, Kyoto University. His current interests involve artificial photosynthesis, photofunctional materials, self-assembly, and porphyrin and fullerene chemistry. He has been a project leader of a PRESTO project of the Japan Science and Technology Agency (JST) since 2001. To date, Hiroshi Imahori has written more than 110 original papers.

Hiroshi Imahori

ism or a one-step superexchange mechanism. The energy of $(Bchl)_2^{\bullet+}Bphe^{\bullet-}$ (~1.2 eV) is lowered by ~0.2 eV, which matches well the reorganization energy (λ) of ET to optimize the forward ET process, but the charge recombination (CR) process is shifted deeply into the inverted region of Marcus parabola to retard the CR process. In a subsequent charge-shift (CSH) step, an electron is transferred in ~200 ps from $Bphe^{\bullet-}$ to the primary quinone Q_A, over R_{ee} value of ~9 Å. This reaction yields the charge-separated state of $(Bchl)_2^{\bullet+}Q_A^{\bullet-}$, which lies only ~0.6 eV above the ground state. This implies that an energy as large as 0.8 eV is lost to obtain the charge-separated state. In a final isoenergetic step, an ET takes place from $Q_A^{\bullet-}$ to Q_B, with a time constant of ~100 μs. The resulting final charge-separated state, which exhibits a total quantum efficiency of nearly 100% as well as a lifetime of the order of seconds across the membrane, eventually leads to production of chemical energy.[2,3] The unique, nano-sized three-dimensional structure and the novel function as a solar energy conversion system have inspired many synthetic chemists during the last two decades. Synthetic methods allow us to modulate photoinduced energy and electron transfer processes in donor–acceptor systems by connecting the donors and the acceptors covalently, instead of embedding them into protein matrices. Therefore, toward the final goal of practical solar energy conversion and the exploitation of photonic molecular devices, donor–bridge–acceptor molecules have been synthesized to elucidate the controlling factors for photosynthetic energy and electron transfer.[1,4–7] In this review, we describe the porphyrin–fullerene-based strategy for the construction of artificial photosynthetic mimics and devices. In particular, porphyrins and fullerenes are shown to be excellent building blocks in the construction of photoinduced electron transfer systems through our studies.

2 Photoinduced single-step electron transfer *versus* multi-step electron transfer

Let us think about the difference between photoinduced single-step electron transfer (PISET) and photoinduced multi-step electron transfer (PIMET). In the case of PISET, the photo-excitation of a donor or an acceptor results in formation of a donor radical cation and an acceptor radical anion, which in turn undergo CR to regenerate the initial state. Since PISET consists of single, short-range ET process, it can minimize losing the input photon energy, some of which would be lost in the case of multi-step electron transfer. Unfortunately, under the PISET conditions the electronic coupling between the resulting donor radical cation and acceptor radical anion is intense so that, in general, the charge recombination takes place rapidly.[8] On the other hand, PIMET is employed as a key strategy in natural photosynthesis (*vide supra*). Although PIMET leads to a substantial loss of the input photon energy by each electron transfer process, the resulting distantly separated radical ion pair attenuates the electronic coupling significantly, thereby prolonging the lifetime of a final charge-separated state. In addition, if the ET efficiency in each process is nearly 100%, the total ET efficiency would be also ~100%, as attained in photosynthetic reaction center.

One also has to modulate reorganization energy, one of the key parameters, for the optimization of photoinduced charge separation (CS) and CR processes. The reorganization energy (λ) is divided into an internal term λ_i involving vibrational energy changes between the reactant and product states and a solvent term λ_s involving the solvent orientation and polarization.[8] The solvent reorganization energy is a function of radius of donor and acceptor, separation distance, and solvent polarity. In particular, the Marcus theory of ET predicts that reorganization energy decreases with decreasing the separation distance between donor and acceptor.[8] Although in the case of a short separation distance the electronic coupling between the donor and the acceptor is large, the photoinduced CS process

and the CR process would be manipulated to be near the Marcus top region and deeply into the Marcus inverted region, respectively, by matching the free energy change for the CS process ($-\Delta G_{CS}$) with the λ value ($-\Delta G_{CS} \sim \lambda$) and making the free energy change for the CR process ($-\Delta G_{CR}$) much larger than the λ value ($-\Delta G_{CR} \gg \lambda$). Therefore, it is a matter of great importance to select a donor–acceptor pair not only with suitable redox potentials and excitation energies, but also with suitably small reorganization energies, which would accelerate photoinduced charge separation and retard charge recombination. In addition, a sensitizer should harvest intensively the visible light (400–800 nm), which corresponds to the main distribution of the solar light spectrum on the earth. Along this line, we have demonstrated that porphyrins[9] as a donor as well as a sensitizer and fullerenes[10] as an acceptor are ideal components for realizing fast photoinduced CS and slow CR compared with conventional donor–acceptor couples, as a result of the small reorganization energies of porphyrins and fullerenes.[7,11,12]

3 Photoinduced single-step electron transfer in porphyrin–fullerene linked dyads

We have prepared a variety of porphyrin and chlorin-fullerene linked dyads with different spacers to disclose the photo-dynamical properties.[11,13–34] As a representative example, the photodynamics of zinc porphyrin–C_{60} linked dyad $\mathbf{1}$.[19–22] and free-base porphyrin-C_{60} linked dyad $\mathbf{2}$ [19,22] are presented (Fig. 1). For instance, photoexcitation of $\mathbf{1}$ in polar solvents (*i.e.*, PhCN, absorption ratio of ZnP : C_{60} = 77 : 23 at 532 nm) results in the occurrence of a photoinduced electron transfer, evolving all the excited states, that is, from $^1ZnP^*$ ($k_{ET(CS1)} = 9.5 \times 10^9$ s^{-1}) and $^3ZnP^*$ ($k_{ET(CS4)} > 1.5 \times 10^7$ s^{-1}) to C_{60} and from ZnP to $^1C_{60}^*$ ($k_{ET(CS2)} = 5.5 \times 10^8$ s^{-1}) and $^3C_{60}^*$ ($k_{ET(CS3)} = 1.5 \times 10^7$ s^{-1}), yielding the same charge-separated state ($ZnP^{\bullet+}$–$C_{60}^{\bullet-}$). The energy levels in PhCN are shown in Scheme 1 to illustrate the different relaxation pathways of photoexcited $\mathbf{1}$.[19–22] The CS efficiencies from $^1ZnP^*$ ($\Phi_{CS1}(^1ZnP^*)$) and $^1C_{60}^*$ ($\Phi_{CS2}(^1C_{60}^*)$) were determined to be 95% and 23%, respectively. The unquenched $^1ZnP^*$ and $^1C_{60}^*$ undergo an intersystem crossing to yield $^3ZnP^*$ and $^3C_{60}^*$, respectively, which then generate the charge-separated state quantitatively.[19–22]

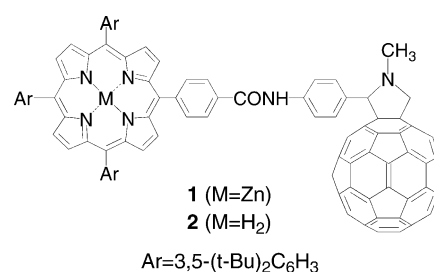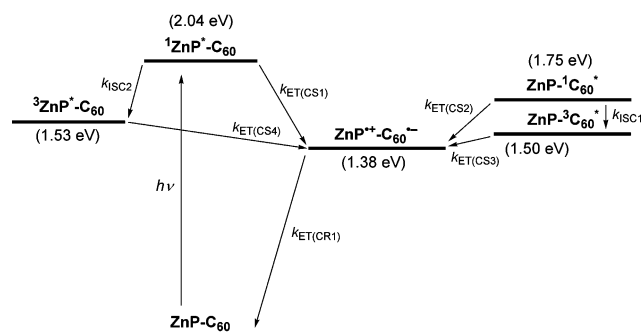Ar=3,5-(t-Bu)$_2$C$_6$H$_3$

Fig. 1 Porphyrin–C_{60} dyads $\mathbf{1}$ (M = Zn) and $\mathbf{2}$ (M = H$_2$).

Scheme 1 Reaction scheme and energy diagram for $\mathbf{1}$ in PhCN.

The total efficiency of $ZnP^{\bullet+}-C_{60}^{\bullet-}$ formation from the initial excited states in PhCN was estimated to be 99% based on Scheme 1. The resulting charge-separated state recombines to regenerate the ground state with a rate constant ($k_{ET(CR1)}$) of 1.3 $\times 10^6$ s^{-1} (0.77 μs) in PhCN. This rate constant is nearly four orders of magnitude smaller than that of the fastest-occurring charge separation, namely, that stemming from $^1ZnP^*$.[19–22] Such fast charge separation and slow charge recombination for **1** in polar solvents is in sharp contrast to conventional porphyrin–quinone, porphyrin–diimide, and diporphyrin linked dyads,[35] where the charge recombination rates are even larger than the charge separation rates in polar solvents.

To quantify the driving force dependence on the ET rate constants (k_{ET}), eqn. (1) was employed, where V is the electronic coupling matrix element, k_B is the Boltzmann constant, h is the Planck constant, and T is the absolute temperature. By fitting the data of the CS and CR processes in polar solvents (THF, PhCN, and DMF) with eqn. (1), the λ and V values of **1** were obtained as $\lambda = 0.66$ eV and $V = 3.9$ cm^{-1}, respectively.[22] It should be noted here that three different kinds of regions in the Marcus curve are seen for **1** explicitly; the charge separation processes from the porphyrin to the singlet and triplet excited states of the C_{60} (Marcus normal region) and from the singlet excited state of the porphyrin to the C_{60} (Marcus top region) and the charge recombination process from the charge-separated state to the ground state (Marcus inverted region).

$$k_{ET} = \left(\frac{4\pi^3}{h^2 \lambda k_B T} \right)^{1/2} V^2 \exp\left[-\frac{(\Delta G^0_{ET} + \lambda)^2}{4 \lambda k_B T} \right] \qquad (1)$$

A similar diagram can be summarized for the free-base porphyrin–C_{60} dyad **2** in PhCN (absorption ratio of $H_2P : C_{60} =$ 83 : 17 at 532 nm) (Scheme 2).[19,22] Photoinduced charge separation from the free-base porphyrin singlet excited state ($^1H_2P^*$ (1.89 eV)) to C_{60} in PhCN occurs to yield $H_2P^{\bullet+}-C_{60}^{\bullet-}$ (1.59 eV) with a rate constant ($k_{ET(CS1)}$) of 6.7×10^8 s^{-1} ($\Phi_{CS1}(^1H_2P^*) =$ 87%). In contrast to the zinc porphyrin–C_{60} dyad **1**, the resulting charge-separated state decays with a rate constant of 5.0×10^7 s^{-1}, generating the porphyrin ($^3H_2P^*$) and fullerene ($^3C_{60}^*$) triplet states rather than the ground state, because the former processes are much faster than the latter process owing to the small reorganization energy of C_{60}. Photoinduced charge separation from the free-base porphyrin to the C_{60} excited singlet state (1.75 eV) may also occur to produce $H_2P^{\bullet+}-C_{60}^{\bullet-}$ (1.59 eV). Unfortunately, however, the CS rate ($k_{ET(CS2)}$) could not be determined by the fluorescence lifetime measurements because of the interference caused by the strong emission (600–750 nm), which overlaps extensively with the much weaker fullerene emission (720 nm). The unquenched $H_2P-{}^1C_{60}^*$ undergoes an intersystem crossing to yield $H_2P-{}^3C_{60}^*$ (1.50 eV), which then decays either to the ground state or to the $^3H_2P^*-C_{60}$ state (1.40 eV).[19,22]
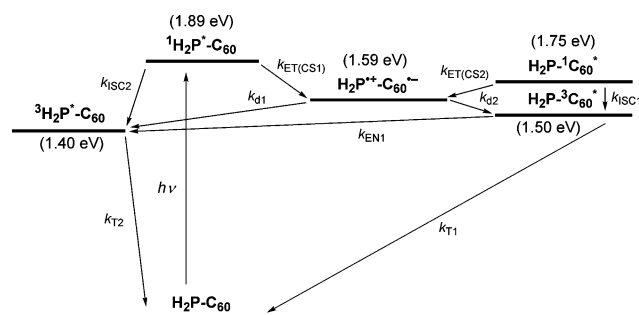
Scheme 2 Reaction scheme and energy diagram for **2** in PhCN.

As expected from the Marcus theory of electron transfer, with decreasing R_{ee} (edge-to-edge distance) value, the solvent reorganization energy and the V value decrease and increase, respectively. Thus, the charge recombination rate would be remarkably slowed down in the case of a small R_{ee} value relative to a large R_{ee} value, provided that the driving forces for charge recombination are similar in the Marcus inverted region. The photophysical properties of zinc chlorin dyads **3**, **4** and free-base chlorin dyad **5** with the same short spacer ($R_{ee} = 5.9$ Å) have been examined to verify the concept (Fig. 2).[24,25]
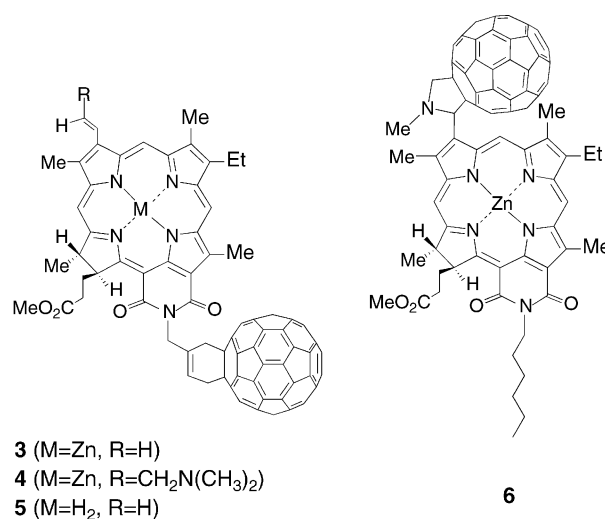

3 (M=Zn, R=H)
4 (M=Zn, R=CH$_2$N(CH$_3$)$_2$)
5 (M=H$_2$, R=H)

6

Fig. 2 Chlorin-C_{60} dyads **3**–**6**.

The photoexcitation of the zinc chlorin–C_{60} dyad results in formation of a long-lived radical ion pair, which has characteristic absorption maxima at 790 and 1000 nm due to the zinc chlorin radical cation and the C_{60} radical anion, respectively. The radical ion pair decays via first-order kinetics with decay rate constants of 9.1×10^3 s^{-1} (110 μs) for **3** and 2.0×10^4 s^{-1} (50 μs) for **4**, which are two orders of magnitude smaller than the value of **1**. On the other hand, the photoexcitation of the free-base chlorin–C_{60} dyad **5** with the same short linkage leads to formation of the radical ion pair which decays quickly to the triplet excited state of the chlorin moiety, as in the case of **2**. The driving force dependence of the electron transfer rate constants of these dyads with a short spacer affords a small reorganization energy ($\lambda = 0.51$ eV) and a large V value (7.8 cm^{-1})[24,25] as compared with the λ (0.66 eV) and V (3.9 cm^{-1}) values of zinc porphyrin–C_{60} dyads with a longer spacer **1** ($R_{ee} =$ 11.9 Å).[22]

The remarkable long-lived charge-separated state of **3** and **4** has prompted us to design the zinc chlorin–fullerene dyad **6** with an extremely short linkage ($R_{ee} = 2.2$ Å), as shown in Fig. 2.[34] Photoexcitation of **6** results in the formation of the ultra-long lived charge-separated state by photoinduced single-step electron transfer by minimizing the loss of input energy, which is inevitable for the charge separation via multi-step electron transfer processes. The lifetime of the charge-separated state of **6** was determined to be 120 s (8.3×10^{-3} s^{-1}) in frozen PhCN at 123 K,[34] which is the longest value of charge separation ever reported for donor–acceptor linked systems.[31,36–42] Unfortunately, however, the quantum yield of formation of the charge-separated state was as low as 12%, which is much smaller than the efficiency of the photoinduced charge separation (100%) estimated from the fluorescence lifetime of the porphyrin moiety. Porphyrin–fullerene dyads and their analogs with a short spacer are known to form a short-lived exciplex via photoinduced ET.[11d,17,26,27,32,42] Some part of the exciplex is converted into a long-lived charge-separated state, whereas the other part of the exciplex decays quickly to the ground state.[17,26,27,32,43] The relative ratio of the decay pathways to the charge-separated state versus to the ground state decreases with decreasing the R_{ee} value due to the larger interaction between the two chromophores in the excited state. The PISET strategy together with shortening the separ-

ation distance between donor and acceptor is highly promising for prolonging the lifetime of a charge-separated state, but the approach does not seem capable of realizing a high quantum yield of formation of the charge-separated state, which would be necessary for the efficient conversion of solar energy into chemical and electrical energies. To realize a high quantum yield of formation of a charge-separated state as well as a long lifetime, we will have to employ an alternative strategy, PIMET.

4 Photodynamics of porphyrin–fullerene linked triads

As we described in the previous section, the combination of porphyrins and their analogs with fullerenes was found to be ideal in donor–acceptor linked systems, because porphyrin–fullerene linked dyads can realize fast photoinduced charge separation and slow charge recombination without a special environment (*i.e.*, protein matrix). Therefore, utilization of porphyrins and fullerenes in multi-step electron transfer systems seems to be a promising strategy to yield a long-lived charge-separated state with a high quantum yield, as seen in the natural reaction center.

We have prepared a variety of porphyrin–fullerene linked triads to mimic photosynthetic multi-step electron transfer.[19,21,22,44–49] One of the representative examples is zinc porphyrin–free-base porphyrin–fullerene triad ($ZnP–H_2P–C_{60}$) **7**, as illustrated in Fig. 3.[19,22,46] The zinc porphyrin attached to free-base porphyrin–C_{60} dyad **2** is designed to exhibit sequential energy transfer and charge separation processes, which mimic both the antenna function in the light-harvesting complex and the subsequent charge separation function in the reaction center (Scheme 3).
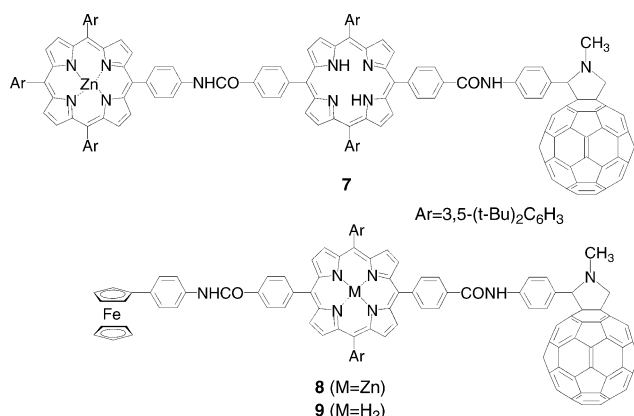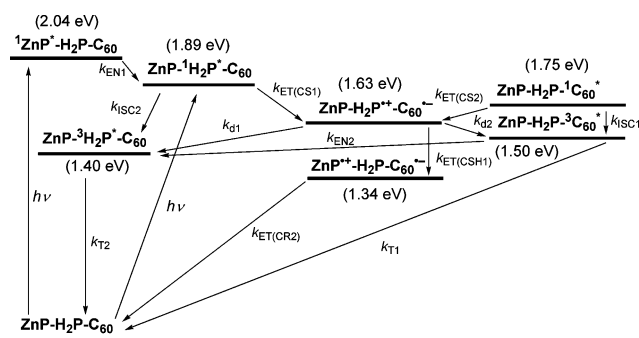

Fig. 3 Zinc porphyrin–free-base porphyrin–C_{60} triad **7** and ferrocene–porphyrin–C_{60} triads **8** (M = Zn) and **9** (M = H_2).

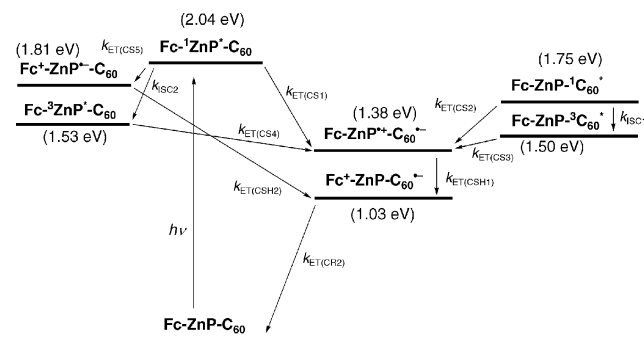**Scheme 3** Reaction scheme and energy diagram for **7** in PhCN.

Photoexcitation of **7** in polar solvents (*i.e.*, PhCN, absorption ratio of ZnP : H_2P : C_{60} = 27 : 61 : 12 at 532 nm) leads to the occurrence of photoinduced EN and ET within the molecule. An initial singlet–singlet energy transfer takes place from $^1ZnP^*$ (2.04 eV) to H_2P (1.89 eV) ($k_{EN1} = 1.5 \times 10^{10}$ s^{-1}, $\Phi_{EN} = 0.97$) to

generate the free-base porphyrin excited singlet state, which is also produced by the direct excitation of the free-base porphyrin moiety. Photoinduced charge separation from the free-base porphyrin to the C_{60} excited singlet state (1.75 eV) also occurs to produce $ZnP–H_2P^{\bullet+}–C_{60}{}^{\bullet-}$ (1.59 eV), whereas the unquenched $ZnP–H_2P–{}^1C_{60}{}^*$ undergoes an intersystem crossing to yield $ZnP–H_2P–{}^3C_{60}{}^*$ (1.50 eV), which then decays either to the ground state or to the $ZnP–{}^3H_2P^*–C_{60}$ state (1.40 eV), as in the case of $H_2P–C_{60}$ (*vide supra*). Then, a sequential electron transfer relay starts from $ZnP–{}^1H_2P^*–C_{60}$ *via* CS1 ($k_{ET(CS1)} = 6.2 \times 10^8$ s^{-1}, $\Phi_{CS1}({}^1H_2P^*) = 0.86$) to yield $ZnP–H_2P^{\bullet+}–C_{60}{}^{\bullet-}$ (1.63 eV). In competition with the decay to the $^3H_2P^*$ state and the $^3C_{60}{}^*$ state, a charge shift occurs from the zinc porphyrin to the free-base porphyrin radical cation to yield $ZnP^{\bullet+}–H_2P–C_{60}{}^{\bullet-}$ (1.34 eV). By analyzing the kinetics of the π-radical cation at 650 nm, the rate constant of the charge-shift reaction was determined to be $k_{ET(CSH1)} = 1.5 \times 10^9$ s^{-1} in PhCN. The final charge-separated state is formed in a moderate quantum yield ($\Phi_{CS(Total)} = 40\%$), which was determined by analyzing the transient absorption spectrum of the $C_{60}{}^{\bullet-}$. The final charge-separated state decays directly to the ground state with a rate constant ($k_{ET(CR2)}$) of 4.8×10^4 s^{-1} (21 μs). The direct decay of $ZnP–H_2P^{\bullet+}–C_{60}{}^{\bullet-}$ to the ground state is negligible because of the slow CR rate (~10^4 s^{-1}) estimated in light of the Marcus theory of ET (*vide supra*).

An additional donor (*i.e.*, ferrocene) was tethered to the porphyrin moiety of zinc porphyrin–C_{60} **1** and of free-base porphyrin–C_{60} **2** to give **8** and **9**, respectively (Fig. 3).[21,22,48] Ferrocene–porphyrin–fullerene triads **8** and **9** are expected to extend the lifetime of a final charge-separated state without lowering the CS efficiency, as diagrammed in Scheme 4 and Scheme 5.

Scheme 4 Reaction scheme and energy diagram for **8** in PhCN.
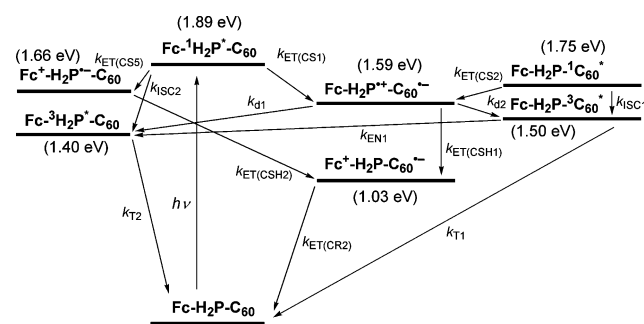
Scheme 5 Reaction scheme and energy diagram for **9** in PhCN.

Based on the energy level of each state for **8** in benzonitrile (absorption ratio of Fc : ZnP : C_{60} = 1 : 75 : 24 at 532 nm), initial photoinduced charge separation occurs from all of the excited states to produce the same charge-separated state (Fc–$ZnP^{\bullet+}$–$C_{60}{}^{\bullet-}$ (1.38 eV)); these are, from the porphyrin singlet excited state $^1ZnP^*$ ($k_{ET(CS1)} = 9.5 \times 10^9$ s^{-1}, $\Phi_{CS1}({}^1ZnP^*) = 90\%$) and porphyrin triplet excited state $^3ZnP^*$ ($k_{ET(CS4)} > 3.2 \times 10^6$ s^{-1}, $\Phi_{CS4}({}^3ZnP^*) > 99\%$) to the C_{60} moiety, and from the porphyrin moiety to the C_{60} singlet excited state $^1C_{60}{}^*$ ($k_{ET(CS2)} = 5.1 \times 10^8$

s^{-1}, $\Phi_{CS2}(^1C_{60}*) = 40\%$) and the C_{60} triplet excited state $^3C_{60}*$ ($k_{ET(CS3)} = 3.2 \times 10^6$ s^{-1}, $\Phi_{CS3}(^3C_{60}*) = 99\%$), as in the case of **1** (*vide supra*). The resulting transient $Fc–ZnP^{\bullet+}–C_{60}^{\bullet-}$ state undergoes a subsequent charge shift to yield the final charge-separated state ($Fc^+–ZnP–C_{60}^{\bullet-}$) with a rate constant of 2.8×10^9 s^{-1} in PhCN. The efficiency of charge shift from Fc to $ZnP^{\bullet+}$ in $Fc–ZnP^{\bullet+}–C_{60}^{\bullet-}$ was found to be nearly unity. Although the small molar coefficient of the ferricenium ion (800 nm) precludes the direct detection of the formation of Fc^+, exclusive decay of the $ZnP^{\bullet+}$ fingerprint at 650 nm in $Fc–ZnP^{\bullet+}–C_{60}^{\bullet-}$ allows us to conclude the formation of the final charge-separated state. Another minor CS process occurs from the ferrocene to the $^1ZnP*$ to produce $Fc^+–ZnP^{\bullet-}–C_{60}$ ($k_{ET(CS5)} = 5.5 \times 10^8$ s^{-1}, $\Phi_{CS5}(^1ZnP*) = 5\%$), followed by a charge shift to yield $Fc^+–ZnP–C_{60}^{\bullet-}$ quantitatively. Totally, the overall quantum yield of formation of the final charge-separated state was determined to be 99% based on Scheme 4. By analyzing the decay kinetics of the $C_{60}^{\bullet-}$ fingerprint at 1000 nm, the electron transfer rate constant for charge recombination in $Fc^+–ZnP–C_{60}^{\bullet-}$ was determined to be 1.3×10^5 s^{-1} (7.7 μs) in PhCN. Therefore, ferrocene–zinc porphyrin–fullerene triad **8** can generate a relatively long-lived charge-separated state with an extremely high quantum yield.[21,22,48]

$Fc–H_2P–C_{60}$ **9** exhibits similar photodynamical behavior in PhCN (absorption ratio of $Fc : H_2P : C_{60} = 1 : 86 : 13$ at 532 nm), as shown in Scheme 5. First, an initial electron transfer to C_{60} ($k_{ET(CS1)} = 1.4 \times 10^9$ s^{-1}, $\Phi_{CS1}(^1H_2P*) = 53\%$) follows the instantaneous population of $Fc–^1H_2P*–C_{60}$ (1.89 eV), to yield $Fc–H_2P^{\bullet+}–C_{60}^{\bullet-}$ (1.59 eV). The resulting charge-separated state decays *via* three different pathways with respective rate constants, namely, i) (k_{d1}) to $Fc–^3H_2P*–C_{60}$ (1.40 eV), ii) (k_{d2}) to $Fc–H_2P–^3C_{60}*$ (1.50 eV), and iii) ($k_{ET(CSH1)}$) to $Fc^+–H_2P–C_{60}^{\bullet-}$ (1.03 eV). The quantum yield of formation of the final charge-separated state was as low as 25%, which was determined by using the transient absorption spectrum of $C_{60}^{\bullet-}$. The lifetime (8.3 μs) in PhCN is comparable to that of **8**. Although the direct detection of the formation of Fc^+ was unsuccessful as a result of the small molar coefficient of the ferricenium ion (800 nm), the long lifetime (8.3 μs) relative to $H_2P–C_{60}$ supports the formation of the final charge-separated state. Photoinduced charge separation from the free-base porphyrin to the C_{60} excited singlet state (1.75 eV) may also take place to produce $Fc–H_2P^{\bullet+}–C_{60}^{\bullet-}$. Unfortunately, however, the CS rate ($k_{ET(CS2)}$) could not be obtained by the fluorescence lifetime measurements because of the weak fullerene emission (*vide supra*). The unquenched $Fc–H_2P–^1C_{60}*$ undergoes an intersystem crossing to yield $Fc–H_2P–^3C_{60}*$ (1.50 eV), which then decays either to the ground state or to the $Fc–^3H_2P*–C_{60}$ state (1.40 eV),[21,22] as in the case of $H_2P–C_{60}$ (*vide supra*). Another CS occurs from the ferrocene to the $^1H_2P*$ to produce $Fc^+–H_2P^{\bullet-}–C_{60}$ ($k_{ET(CS5)} = 6.1 \times 10^8$ s^{-1}, $\Phi_{CS5}(^1H_2P*) = 40\%$), followed by a charge shift to yield $Fc^+–H_2P–C_{60}^{\bullet-}$.

The best fits of eqn. (1) provide $\lambda = 1.09$ eV and $V = 0.019$ cm^{-1} for the charge recombination process of the triad systems **7–9** in polar solvents. It should be emphasized here that both the normal and inverted regions of the Marcus parabola have been observed for the first time for intramolecular charge recombination processes in the covalently linked triads. These examples clearly demonstrate that C_{60} is a suitable component for the construction of photoinduced multi-step electron transfer systems.

5 Photodynamics of porphyrin–fullerene linked tetrads

To further prolong the lifetime of the final charge-separated state, we have designed a ferrocene (Fc)–zinc porphyrin (ZnP)–free-base porphyrin (H_2P)–C_{60} tetrad **10**.[39] Taking into account the similarity in molecular structures of **7**, **8**, and **10**, we can anticipate the photodynamical behavior of **10** from that of **7**

and **8** (Scheme 6). Thus, the lifetime of the charge-separated state is expected to be improved remarkably without lowering the efficiency of charge separation, because the eventual charges ($Fc^+–ZnP–H_2P–C_{60}^{\bullet-}$) are separated by $R_{ee} = 48.9$ Å.

The picosecond transient spectroscopic measurements revealed that an efficient singlet–singlet energy transfer ($k_{EN1} \sim 3 \times 10^9$ s^{-1}, $\Phi_{EN} \sim 83\%$), stemming from the initially excited $^1ZnP*$ to the adjacently located and energetically lower-lying $^1H_2P*$, governs the rapid deactivation of $^1ZnP*$ (absorption ratio of $Fc : ZnP : H_2P : C_{60} = 1 : 25 : 57 : 17$ at 532 nm in PhCN). From this $^1H_2P*$ state, a rapid intramolecular electron transfer occurs with a rate constant of $k_{ET(CS1)} = 6.2 \times 10^8$ s^{-1} ($\Phi_{CS1}(^1H_2P*) = 86\%$) to yield the primary radical ion pair state ($Fc–ZnP–H_2P^{\bullet+}–C_{60}^{\bullet-}$). The primary radical ion pair is then a starting point for a cascade of short-range charge-shift reactions along a well-tuned redox gradient. Namely, time profiles, which unravel both the formation ($ZnP^{\bullet+}$) and the decay ($H_2P^{\bullet+}$) kinetics with the same time constant ($k_{ET(CSH1)} = 2.5 \times 10^9$ s^{-1}) at 650 nm and 555 nm, respectively, corroborate the subsequent formation of $Fc–ZnP^{\bullet+}–H_2P–C_{60}^{\bullet-}$, the transient of which is identical with that of $ZnP^{\bullet+}–H_2P–C_{60}^{\bullet-}$. The rate constant of the second charge shift could be derived from the decay of the time-profile at 650 nm ($k_{ET(CSH2)} = 1.7 \times 10^8$ s^{-1}). The two successive charge shifts create eventually the spatially separated radical ion pair ($Fc^+–ZnP–H_2P–C_{60}^{\bullet-}$) with a total quantum yield of 24% (PhCN), which was determined from the transient absorption spectrum of $C_{60}^{\bullet-}$.[39] The transient absorption of $Fc^+–ZnP–H_2P–C_{60}^{\bullet-}$ bears no spectral resemblance to the intermediate species, supporting formation of the final charge-separated state. A similar diagram can be summarized for the deactivation pathway of the C_{60} excited singlet state, as in the case of $H_2P–C_{60}$ and $ZnP–H_2P–C_{60}$ (*vide supra*).

In contrast to the case of the dyad **1** and triads **7–9**, the decay dynamics of the charge-separated radical pair ($Fc^+–ZnP–H_2P–C_{60}^{\bullet-}$), followed by use of the time profile at 1000 nm in various polar solvents, obeys second-order kinetics rather than first-order kinetics. This indicates that the intramolecular electron transfer is too slow to be observed in competition with the diffusion-limited intermolecular electron transfer from $C_{60}^{\bullet-}$ in one tetrad to Fc^+ in another tetrad in fluid solvents. To preclude the *inter*molecular electron transfer against *intra*molecular electron transfer processes in $Fc^+–ZnP–H_2P–C_{60}^{\bullet-}$, electron spin resonance (ESR) measurements were performed in frozen PhCN (1.0×10^{-5} M) of **10** at various temperatures under photoirradiation. The ESR spectrum shows a characteristic broad signal of the $C_{60}^{\bullet-}$ ($g = 2.0004$) at 163 K under the irradiation. The lack of appearance of the ferricenium ion (Fc^+) in the ESR spectrum of **10** is supported by the fact that Fc^+ itself exhibits no significant ESR signal under the same conditions, due to the fast relaxation of the signal. The ESR signal appeared immediately upon irradiation of the frozen PhCN solution of **10** and fell slowly with a rate constant ($k_{ET(CR3)}$) of 2.6 s^{-1} (0.38 s at 163 K) *via* first-order kinetics when the irradiation was turned off. This clearly shows that the ESR signal of **10** results largely from intramolecular radical ion pair ($Fc^+–ZnP–H_2P–C_{60}^{\bullet-}$). From the analysis of temperature dependence of the ET rate constants, the reorganization energy (λ) and electronic coupling matrix element (V) were determined as 1.37 eV and 1.6×10^{-4} cm^{-1} in PhCN.[39] The electron transfer rate constants ($k_{ET(optimal)}$) of the tetrad (**10**, $R_{ee} = 48.9$ Å), triad (**7–9**, $R_{ee} = 30.3$ Å), and dyad (**1**, $R_{ee} = 11.9$ Å) systems in the top region of the Marcus curve are correlated with the edge-to-edge distance (R_{ee}) according to eqn. (2),

$$\ln(k_{ET(optimal)}) = \ln\left(\frac{2\pi^{3/2}V_0^2}{h(\lambda k_B T)^{1/2}}\right) - \beta R_{ee} \qquad (2)$$

where V_0 is the maximal electronic coupling element and β is the decay coefficient factor (damping factor), which depends primarily on the nature of the bridge molecule. The β value
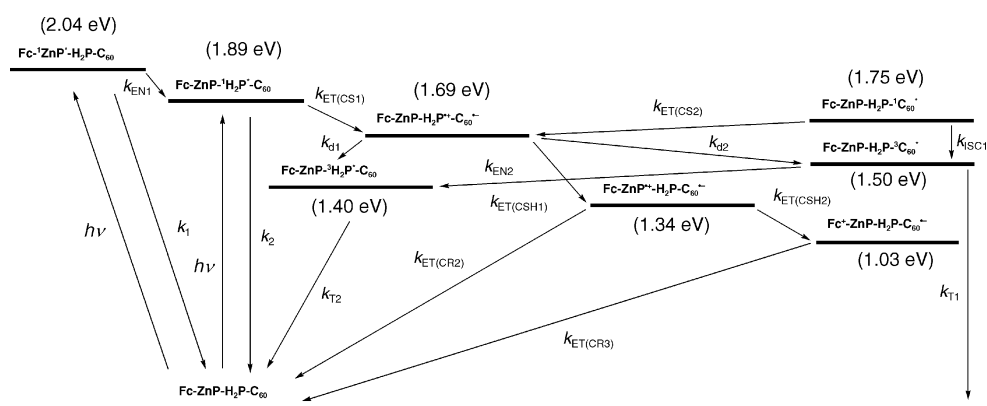
Scheme 6 Reaction scheme and energy diagram for **10** in PhCN.
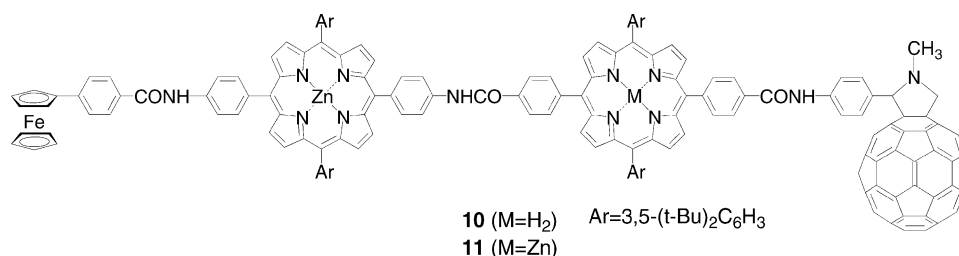
Fig. 4 Ferrocene–zinc porphyrin–free-base porphyrin–C_{60} tetrad **10** and ferrocene–zinc porphyrin–zinc porphyrin–C_{60} tetrad **11**.
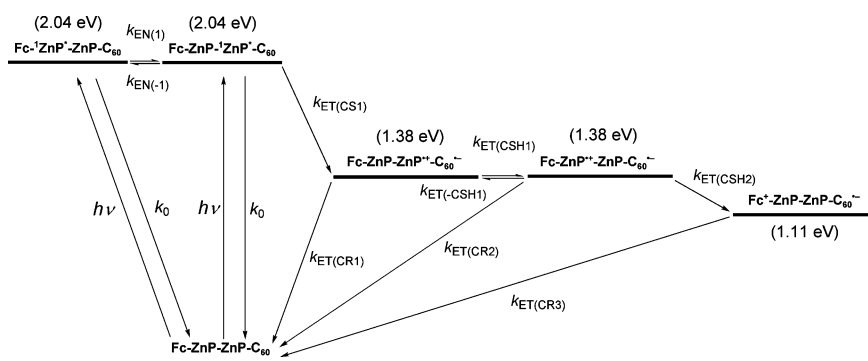
Scheme 7 Reaction scheme and energy diagram for **11** in PhCN.

$(0.60\ \text{Å}^{-1})$ is located within a boundary of nonadiabatic electron transfer reactions for saturated hydrocarbon bridges $(0.8–1.0\ \text{Å}^{-1})$ and unsaturated phenylene bridges $(0.4\ \text{Å}^{-1})$.[50]

These results clearly demonstrate that the intramolecular charge recombination process of **10** was observed successfully by the ESR measurements under the photoirradiation. The lifetime (0.38 s at 163 K in PhCN) is the longest one ever reported for intramolecular charge recombination in donor–acceptor linked molecules using photoinduced multi-step ET. More importantly, the value is comparable to the lifetimes ($\sim$1 s^{-1}) of bacteriochlorophyll dimer radical cation $((\text{Bchl})_2^{\bullet+})$–secondary quinone radical anion $(Q_B^{\bullet-})$ ion pair in bacteria photosynthetic reaction centers. In the case of ferrocene–zinc porphyrin–zinc porphyrin–fullerene tetrad **11**[40] (Fig. 4), where a zinc atom is inserted into the free-base porphyrin moiety of **10**, the radical ion pair, $Fc^+–ZnP–ZnP–C_{60}^{\bullet-}$, produced by photoinduced electron transfer (Scheme 7), was detected by means of transient absorption spectra as well as the ESR spectra. The lifetime of a final charge-separated state in **11** (1.6 s in DMF at 163 K) has been further prolonged, compared with that of **10**, under the similar experimental conditions for **10**. The λ value of $Fc^+–ZnP–ZnP–C_{60}^{\bullet-}$ ($\lambda = 1.16$ eV) in DMF is similar to that of $Fc^+–ZnP–H_2P–C_{60}^{\bullet-}$ ($\lambda = 1.27$ eV), because the electron donor $(C_{60}^{\bullet-})$ and acceptor (Fc^+) moieties are the same in $Fc^+–ZnP–ZnP–C_{60}^{\bullet-}$ and $Fc^+–ZnP–H_2P–C_{60}^{\bullet-}$. In contrast, the V value of $Fc^+–ZnP–ZnP–C_{60}^{\bullet-}$ ($V = 5.6 \times 10^{-5}$ cm^{-1}) in DMF is significantly smaller than that of $Fc^+–ZnP–$

$H_2P–C_{60}^{\bullet-}$ ($V = 1.9 \times 10^{-4}$ cm^{-1}). Such a smaller V value may result from the smaller orbital overlap between ZnP and $C_{60}^{\bullet-}$ in $Fc^+–ZnP–ZnP–C_{60}^{\bullet-}$ than that between H_2P and $C_{60}^{\bullet-}$ in $Fc^+–ZnP–H_2P–C_{60}^{\bullet-}$ because of the higher LUMO level (lower E^0_{red}) of the zinc porphyrin compared to the free-base porphyrin. The present far distant radical ion pair is formed with a total quantum yield of 34%. It should be emphasized here that both the lifetime and the quantum yield of the final charge-separated state are improved in **11** relative to the corresponding ferrocene–zinc porphyrin–free-base porphyrin–fullerene tetrad **10**.

6 Photodynamics of ferrocene–porphyrin oligomer–fullerene linked systems

We have achieved the longest-lived charge-separated state in the ferrocene–zinc porphyrin–zinc porphyrin–fullerene (**Fc–ZnP–ZnP–C$_{60}$** in Fig. 4) tetrad, which reveals a cascade of photoinduced energy transfer and multi-step electron transfer within a molecule in frozen media as well as in solutions. The lifetime of the resulting charge-separated state (*i.e.*, ferricenium ion–C_{60} radical anion pair) in a frozen PhCN is as long as 1.6 s, which is comparable to that observed for the bacterial photosynthetic reaction center.[40] However, the quantum yield of formation of the charge-separated state (34%) is still much lower than that of the natural system (100%). Thus, the charge separation

efficiency remains to be much improved. Moreover, the light-harvesting efficiency should also be enhanced. In this context, *meso*,*meso*-porphyrin arrays are good candidates to improve both efficiencies, since the length of *meso*,*meso*-porphyrin arrays can be extended easily by facile oligomerization of the porphyrin monomer.[51] In addition, they can collect visible light more widely than a linear combination of the corresponding porphyrin monomer due to the exciton coupling of the porphyrins, as seen in molecular assemblies of chlorophylls in antenna complex.[2,3]

First, we have incorporated *meso*-,*meso*-linked porphyrin dimer [$(ZnP)_2$] as an improved light-harvesting chromophore, instead of porphyrin monomer, into photosynthetic ET model **8** to construct the ferrocene–*meso*,*meso*-linked porphyrin dimer–fullerene tetrad **12** (Fc–$(ZnP)_2$–C_{60}) where the C_{60} and the ferrocene (Fc) are tethered at both the ends of $(ZnP)_2$ (Fig. 5).[52] Photoirradiation of **12** in PhCN (530 nm) results in photoinduced electron transfer from the singlet excited state of the porphyrin dimer [$^1(ZnP)_2*$] to the C_{60} moiety to produce the porphyrin dimer radical cation–C_{60} radical anion pair Fc–$(ZnP)_2^{\bullet+}$–$C_{60}^{\bullet-}$ ($k_{ET(CS1)} = 5.0 \times 10^9$ s^{-1}, $\Phi_{CS1}(^1ZnP*) = 85\%$). The excitation of $(ZnP)_2$ is exclusive under the conditions. The unquenched $^1(ZnP)_2*$ may undergo intersystem crossing to yield $^3(ZnP)_2*$, which is converted into Fc–$(ZnP)_2^{\bullet+}$–$C_{60}^{\bullet-}$ quantitatively. In competition with the back electron transfer from $C_{60}^{\bullet-}$ to $(ZnP)_2^{\bullet+}$ to the ground state ($k_{ET(CR1)} = 1.9 \times 10^6$ s^{-1}), an electron transfer from Fc to $(ZnP)_2^{\bullet+}$ ($k_{ET(CSH1)} = 1.3 \times 10^7$ s^{-1}, $\Phi_{CSH1} = 87\%$) occurs to give the final charge-separated state (Fc$^+$–$(ZnP)_2$–$C_{60}^{\bullet-}$). Another CS occurs from the Fc moiety to the porphyrin dimer to yield Fc$^+$–$(ZnP)_2^{\bullet-}$–C_{60} ($k_{ET(CS2)} = 3.5 \times 10^8$ s^{-1}, $\Phi_{CS2}(^1ZnP*) = 6\%$), followed by the charge shift from the $(ZnP)_2^{\bullet-}$ to the C_{60} to generate the final charge-separated state quantitatively. The total quantum yield of formation of the final charge-separated state was determined to be 88% in benzonitrile on a basis of Scheme 8. The final charge-separated state decays obeying first-order kinetics with a lifetime of 19 μs (5.3×10^4 s^{-1}) in PhCN at 295 K. The lifetime is far shorter than the value expected from the long edge-to-edge distance ($R_{ee} = 38.6$ Å) as compared to the R_{ee} value of Fc$^+$–ZnP–$C_{60}^{\bullet-}$ radical ion pair ($R_{ee} = 30.3$ Å), which has a lifetime of 7.7 μs in PhCN. The activation energy for the charge recombination process was determined to be 0.15 eV in benzo-

nitrile, which is much larger than the value expected from the direct charge recombination process to the ground state. This value is rather comparable to the energy difference between the initial charge-separated state (Fc–$(ZnP)_2^{\bullet+}$–$C_{60}^{\bullet-}$) and the final charge-separated state (Fc$^+$–$(ZnP)_2$–$C_{60}^{\bullet-}$). This suggests that the back electron transfer to the ground state takes place *via* the reversed stepwise processes, *i.e.*, a rate-limiting electron transfer from $(ZnP)_2$ to Fc$^+$ to give the initial charge-separated state (Fc–$(ZnP)_2^{\bullet+}$–$C_{60}^{\bullet-}$), followed by a fast electron transfer from $C_{60}^{\bullet-}$ to $(ZnP)_2^{\bullet+}$ to regenerate the ground state, Fc–$(ZnP)_2$–C_{60}. This is in sharp contrast with the extremely slow direct charge recombination from $Q_B^{\bullet-}$ to $(Bchl)_2^{\bullet+}$ in the bacterial reaction centers, where 60% of the input energy is lost to avoid the stepwise back electron transfer.[2,3]

A *meso*-,*meso*-linked porphyrin trimer [$(ZnP)_3$] as a light-harvesting chromophore has been also incorporated into a photosynthetic multi-step electron transfer model **8** including ferrocene (Fc) as an electron donor and fullerene (C_{60}) as an electron acceptor to construct the ferrocene–*meso*,*meso*-linked porphyrin trimer–fullerene system **13** (Fc–$(ZnP)_3$–C_{60}).[41] The light harvesting efficiency in the visible region is much improved in Fc–$(ZnP)_3$–C_{60} due to the exciton coupling in the porphyrin trimer as well as an increase in the number of the porphyrins. Photoirradiation of Fc–$(ZnP)_3$–C_{60} in PhCN (560 nm) results in photoinduced electron transfer from both the singlet excited state ($k_{ET(CS1)} = 2.7 \times 10^9$ s^{-1}, $\Phi_{CS1}(^1(ZnP)_3*) = 81\%$) and triplet excited state ($k_{ET(CS3)} = 2.5 \times 10^7$ s^{-1}, $\Phi_{CS3}(^1(ZnP)_3*) = 100\%$) of the porphyrin trimer [$^1(ZnP)_3*$, $^3(ZnP)_3*$] to the C_{60} moiety to produce the porphyrin trimer radical cation–C_{60} radical anion pair (Fc–$(ZnP)_3^{\bullet+}$–$C_{60}^{\bullet-}$). The excitation of $(ZnP)_3$ is exclusive under the conditions. In competition with CR from $C_{60}^{\bullet-}$ to $(ZnP)_3^{\bullet+}$ to the ground state ($k_{ET(CR1)} = 1.5 \times 10^6$ s^{-1}), an electron transfer from Fc to $(ZnP)_3^{\bullet+}$ ($k_{ET(CSH1)} = 5.2 \times 10^6$ s^{-1}, $\Phi_{CSH1} = 78\%$) occurs to give the final charge-separated state (Fc$^+$–$(ZnP)_3$–$C_{60}^{\bullet-}$) (Scheme 9). Another minor CS process occurs from the Fc moiety to the porphyrin trimer excited singlet state to yield Fc$^+$–$(ZnP)_3^{\bullet-}$–C_{60} ($k_{ET(CS2)} = 8.9 \times 10^7$ s^{-1}, $\Phi_{CS2}(^1ZnP*) = 3\%$), followed by the charge shift from the $(ZnP)_2^{\bullet-}$ to the C_{60} to generate the final charge-separated state quantitatively. The total quantum yield of formation of the final charge-separated state was determined to be 83% in benzonitrile by using transient absorption spectrum of $C_{60}^{\bullet-}$. The final charge-separated state decays obeying first-order kinetics with a lifetime of 0.53 s (1.9 s^{-1}) in frozen DMF at 163 K.[41] Such a long lifetime of the charge-separated state is comparable with that of the natural bacterial photosynthetic reaction center. More importantly, the quantum yield of formation of the final charge-separated state (*i.e.*, 83% in benzonitrile) remains high despite the large separation distance between the Fc$^+$ and $C_{60}^{\bullet-}$ moieties. The remarkably high quantum yield results from the efficient charge separation through the porphyrin trimer, whereas a slow charge recombination is associated with the localized porphyrin radical cation in the porphyrin trimer. This is in sharp contrast with the rather short lifetime of Fc$^+$–$(ZnP)_2$–$C_{60}^{\bullet-}$ **12** which is related to the delocalized radical cation in the porphyrin dimer.[53]

12 (n=2)
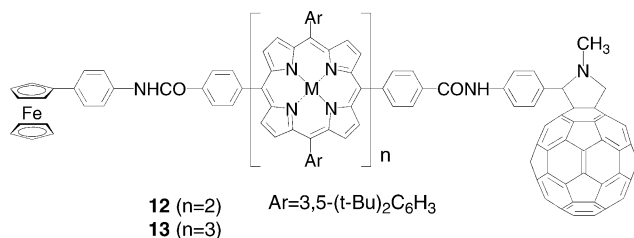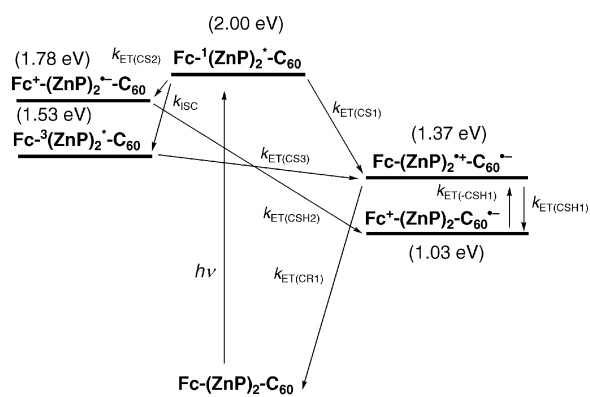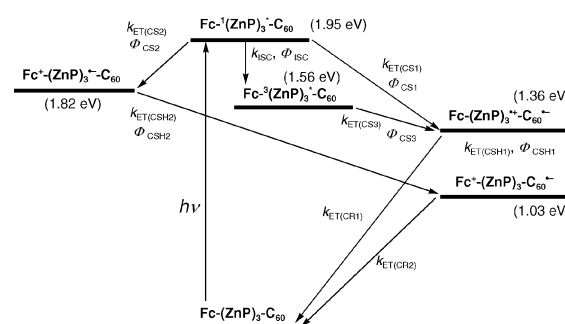**13** (n=3)   Ar=3,5-(t-Bu)$_2$C$_6$H$_3$

Fig. 5 Ferrocene–zinc porphyrin oligomer–C_{60} linked tetrad **12** and pentad **13**.

Scheme 8 Reaction scheme and energy diagram for **12** in PhCN.

Scheme 9 Reaction scheme and energy diagram for **13** in PhCN.

7 Conclusion and outlook

Porphyrins and fullerenes have been found to be excellent building blocks as artificial photosynthetic models by examining photoinduced intramolecular electron transfer in the porphyrin–fullerene linked systems using time-resolved spectroscopic methods covering from picosecond to second time regions. We have proposed and demonstrated, for the first time, that the acceleration and deceleration effects of fullerenes result from their small reorganization energies as compared to those of conventional planar acceptors. The porphyrin–fullerene linked triads, tetrads, and pentad display stepwise electron transfer relay, mimicking the primary charge separation in the photosynthetic reaction center together with the antenna function. In particular, highly efficient photosynthetic electron transfer has been realized in the ferrocene–zinc porphyrin–C_{60} triad, in which the relatively long-lived charge-separated state (up to 16 μs) can be produced with an extremely high quantum yield (nearly unity). More importantly, the ferrocene–zinc porphyrin trimer–fullerene pentad exhibits not only the longest lifetime (0.53 s in PhCN at 163 K) of the charge-separated state ever reported for intramolecular charge recombination in donor–acceptor linked molecules using multistep electron transfer, but also an extremely high CS efficiency (83%), which is comparable to the ET properties of bacteriochlorophyll dimer radical cation ($(Bchl)_2^{\bullet+}$)–secondary quinone radical anion ($Q_B^{\bullet-}$) ion pair in the bacteria photosynthetic reaction center. These results clearly show that porphyrins and fullerenes are good building components for the construction of artificial photosynthetic multicomponent systems.

Applying our novel strategies to construct solar energy conversion systems has been carried out in self-assembled monolayers on metal nanoclusters as well as gold and ITO electrodes.[53–63] Our approach using porphyrin and fullerenes as well as molecular technologies on electrodes using self-assembly will open a door to the development of photoactive molecular devices and machines as well as novel organic solar cells.

References

1 (a) *Molecular Devices and Machines*, ed. V. Balzani, M. Venturi and A. Credi, Wiley-VCH, Weinheim, 2003; (b) *Electron Transfer in Chemistry*, ed. V. Balzani, Wiley-VCH, Weinheim, 2001; (c) *Electron Transfer*, ed. J. Jortner and M. Bixon, John Wiley & Sons, New York, 1999, part 1 and 2; (d) *Molecular Electronics*, ed. J. Jortner and M. Ratner, Blackwell Science, Oxford, 1997; (e) *Organic Photovoltaics*, ed. C. Brabec, V. Dyakonov, J. Parisi and N. S. Sariciftci, Springer, Berlin, 2003; (f) K. Domen, J. N. Kondo, H. Hara and T. Takata, *Bull. Chem. Soc. Jpn.*, 2000, **73**, 1307.

2 (a) *The Photosynthetic Reaction Center*, ed. J. Deisenhofer and J. R. Norris, Academic Press, San Diego, 1993; (b) *Anoxygenic Photosynthetic Bacteria*, ed. R. E. Blankenship, M. T. Madigan and C. E. Bauer, Kluwer Academic Publishing, Dordrecht, 1995; (c) P. A. Loach, *Photochem. Photobiol.*, 1997, **65S**, 134S.

3 (a) G. McDermott, S. M. Prince, A. A. Freer, A. M. Hawthornthwaite-Lawless, M. Z. Papiz, R. J. Cogdell and N. W. Isaacs, *Nature*, 1995, **374**, 517; (b) J. M. Olson, *Photochem. Photobiol.*, 1998, **67**, 61; (c) A. Zouni, H.-T. Witt, J. Kern, P. Fromme, N. Kraub, W. Saenger and P. Orth, *Nature*, 2001, **409**, 739; (d) P. Jordan, P. Fromme, H.-T. Witt, O. Klukas, W. Saenger and N. Kraub, *Nature*, 2001, **411**, 909.

4 (a) M. R. Wasielewski, *Chem. Rev.*, 1992, **92**, 435; (b) D. Gust, T. A. Moore and A. L. Moore, *Acc. Chem. Res.*, 1993, **26**, 198; (c) D. Gust, T. A. Moore and A. L. Moore, *Acc. Chem. Res.*, 2001, **34**, 40; (d) D. Holten, D. F. Bocian and J. S. Lindsey, *Acc. Chem. Res.*, 2002, **35**, 57; (e) D. M. Adams, L. Brus, E. D. Chidsey, S. Creager, C. Creutz, C. R. Kagan, P. V. Kamat, M. Lieberman, J. S. Lindsey, R. A. Marcus, R. M. Metzger, M. E. Michel-Beyerle, J. R. Miller, M. D. Newton, D. R. Rolison, O. Sankey, K. S. Schanze, J. Yardley and X. Zhu, *J. Phys. Chem. B*, 2003, **107**, 6668.

5 (a) H. Kurreck and M. Huber, *Angew. Chem., Int. Ed. Engl.*, 1995, **34**, 849; (b) A. Harriman and J.-P. Sauvage, *Chem. Soc. Rev.*, 1996, **26**, 41; (c) J. W. Verhoeven, *Adv. Chem. Phys.*, 1999, **106**, 603; (d) L. Sun, L. Hammarström, B. Åkermark and S. Styring, *Chem. Soc. Rev.*, 2001, **30**, 36; (e) D. M. Guldi and M. Prato, *Acc. Chem. Res.*, 2000, **33**, 695; (f) N. Armaroli, *Photochem. Photobiol. Sci.*, 2003, **2**, 73.

6 (a) M. N. Paddon-Row, *Acc. Chem. Res.*, 1994, **27**, 18; (b) K. Maruyama, A. Osuka and N. Mataga, *Pure Appl. Chem.*, 1994, **66**, 867.

7 (a) H. Imahori and Y. Sakata, *Adv. Mater.*, 1997, **9**, 537; (b) H. Imahori and Y. Sakata, *Eur. J. Org. Chem.*, 1999, 2445; (c) H. Imahori and S. Fukuzumi, *Adv. Mater.*, 2001, **13**, 1197; (d) H. Imahori, Y. Mori and Y. Matano, *J. Photochem. Photobiol., C*, 2003, **4**, 51; (e) H. Imahori and S. Fukuzumi, *Adv. Funct. Mater.*, 2004, **14**, in press; (f) H. Imahori, *J. Phys. Chem. B*, 2004, **108**, in press.

8 (a) R. A. Marcus, *Annu. Rev. Phys. Chem.*, 1964, **15**, 155; (b) R. A. Marcus and N. Sutin, *Biochim. Biophys. Acta*, 1985, **811**, 265; (c) R. A. Marcus, *Angew. Chem., Int. Ed. Engl.*, 1993, **32**, 1111.

9 *The Porphyrin Handbook*, ed. K. M. Kadish, K. Smith and R. Guilard, Academic Press, San Diego, CA, 2000.

10 (a) *Science of Fullerenes and Carbon Nanotubes*, ed. M. S. Dresselhaus, G. Dresselhaus and P. C. Eklund, Academic Press, San Diego, 1995; (b) *Fullerenes*, ed. K. M. Kadish and R. S. Ruoff, John Wiley & Sons, New York, 2000.

11 (a) H. Imahori, K. Hagiwara, M. Aoki, T. Akiyama, S. Taniguchi, T. Okada, M. Shirakawa and Y. Sakata, *Chem. Phys. Lett.*, 1996, **263**, 545; (b) N. V. Tkachenko, C. Guenther, H. Imahori, K. Tamaki, Y. Sakata, H. Lemmetyinen and S. Fukuzumi, *Chem. Phys. Lett.*, 2000, **326**, 344; (c) H. Imahori, N. V. Tkachenko, V. Vehmanen, K. Tamaki, H. Lemmetyinen, Y. Sakata and S. Fukuzumi, *J. Phys. Chem. A*, 2001, **105**, 1750; (d) V. Vehmanen, N. V. Tkachenko, H. Imahori, S. Fukuzumi and H. Lemmetyinen, *Spectrochim. Acta, Part A*, 2001, **57**, 2229; (e) H. Imahori, H. Yamada, D. M. Guldi, Y. Endo, A. Shimomura, S. Kundu, K. Yamada, T. Okada, Y. Sakata and S. Fukuzumi, *Angew. Chem., Int. Ed.*, 2002, **41**, 2344.

12 S. Fukuzumi, K. Ohkubo, H. Imahori and D. M. Dirk, *Chem. Eur. J.*, 2003, **9**, 1585.

13 H. Imahori, K. Hagiwara, T. Akiyama, S. Taniguchi, T. Okada and Y. Sakata, *Chem. Lett.*, 1995, 265.

14 H. Imahori, K. Hagiwara, M. Aoki, T. Akiyama, S. Taniguchi, T. Okada, M. Shirakawa and Y. Sakata, *J. Am. Chem. Soc.*, 1996, **118**, 11771.

15 H. Imahori and Y. Sakata, *Chem. Lett.*, 1996, 199.

16 K. Yamada, H. Imahori, Y. Nishimura, I. Yamazaki and Y. Sakata, *Chem. Lett.*, 1999, 895.

17 H. Imahori, S. Ozawa, K. Ushida, M. Takahashi, T. Azuma, A. Ajavakom, T. Akiyama, M. Hasegawa, S. Taniguchi, T. Okada and Y. Sakata, *Bull. Chem. Soc. Jpn.*, 1999, **72**, 485.

18 H. Imahori, K. Tamaki, H. Yamada, K. Yamada, Y. Sakata, Y. Nishimura, I. Yamazaki, M. Fujitsuka and O. Ito, *Carbon*, 2000, **38**, 1599.

19 C. Luo, D. M. Guldi, H. Imahori, K. Tamaki and Y. Sakata, *J. Am. Chem. Soc.*, 2000, **122**, 6535.

20 H. Imahori, M. E. El-Khouly, M. Fujitsuka, O. Ito, Y. Sakata and S. Fukuzumi, *J. Phys. Chem. A*, 2001, **105**, 325.

21 S. Fukuzumi, H. Imahori, H. Yamada, M. E. El-Khouly, M. Fujitsuka, O. Ito and D. M. Guldi, *J. Am. Chem. Soc.*, 2001, **123**, 2571.

22 H. Imahori, K. Tamaki, D. M. Guldi, C. Luo, M. Fujitsuka, O. Ito, Y. Sakata and S. Fukuzumi, *J. Am. Chem. Soc.*, 2001, **123**, 2607.

23 H. Imahori, T. Hasobe, H. Yamada, P. V. Kamat, S. Barazzouk, M. Fujitsuka, O. Ito and S. Fukuzumi, *Chem. Lett.*, 2001, 784.

24 S. Fukuzumi, K. Ohkubo, H. Imahori, J. Shao, Z. Ou, G. Zheng, Y. Chen, R. K. Pandey, M. Fujitsuka, O. Ito and K. M. Kadish, *J. Am. Chem. Soc.*, 2001, **123**, 10676.

25 K. Ohkubo, H. Imahori, J. Shao, Z. Ou, K. M. Kadish, Y. Chen, G. Zheng, R. K. Pandey, M. Fujitsuka, O. Ito and S. Fukuzumi, *J. Phys. Chem. A*, 2002, **106**, 10991.

26 T. J. Kesti, N. V. Tkachenko, V. Vehmanen, H. Yamada, H. Imahori, S. Fukuzumi and H. Lemmetyinen, *J. Am. Chem. Soc.*, 2002, **124**, 8067.

27 N. V. Tkachenko, V. Vehmanen, J.-P. Nikkanen, H. Yamada, H. Imahori, S. Fukuzumi and H. Lemmetyinen, *Chem. Phys. Lett.*, 2002, **366**, 245.

28 S. Fukuzumi, H. Imahori, K. Okamoto, H. Yamada, M. Fujitsuka, O. Ito and D. M. Guldi, *J. Phys. Chem. A*, 2002, **106**, 1903.

29 N. Ohta, S. Mikami, Y. Iwaki, M. Tsushima, H. Imahori, K. Tamaki, Y. Sakata and S. Fukuzumi, *Chem. Phys. Lett.*, 2003, **368**, 230.

30 T. Kesti, N. V. Tkachenko, H. Yamada, H. Imahori, S. Fukuzumi and H. Lemmetyinen, *Photochem. Photobiol. Sci.*, 2003, **2**, 251.

31 Kashiwagi, K. Ohkubo, J. A. McDonald, I. M. Blake, M. J. Crossley, Y. Araki, O. Ito, H. Imahori and S. Fukuzumi, *Org. Lett.*, 2003, **5**, 2719.

32 N. V. Tkachenko, H. Lemmetyinen, J. Sonoda, K. Ohkubo, T. Sato, H. Imahori and S. Fukuzumi, *J. Phys. Chem. A*, 2003, **107**, 8834.

33 I. Zilbermann, G. A. Anderson, D. M. Guldi, H. Yamada, H. Imahori and S. Fukuzumi, *J. Porphyrins Phthalocyanines*, 2003, **7**, 357.

34 K. Ohkubo, H. Kotani, J. Shao, Z. Ou, Karl M. Kadish, G. Li, R. K. Pandey, M. Fujitsuka, O. Ito, H. Imahori and S. Fukuzumi, *Angew. Chem., Int. Ed.*, 2004, **43**, 853.

35 (*a*) T. Asahi, M. Ohkohchi, R. Matsusaka, N. Mataga, R. P. Zhang, A. Osuka and K. Maruyama, *J. Am. Chem. Soc.*, 1993, **115**, 5665; (*b*) J. M. DeGraziano, P. A. Liddell, L. Leggett, A. L. Moore, T. A. Moore and D. Gust, *J. Phys. Chem.*, 1994, **98**, 1758; (*c*) A. Osuka, G. Noya, S. Taniguchi, T. Okada, Y. Nishimura, I. Yamazaki and N. Mataga, *Chem. Eur. J.*, 2000, **6**, 33; (*d*) A. Nakano, A. Osuka, T. Yamazaki, Y. Nishimura, S. Akimoto, I. Yamazaki, A. Itaya, M. Murakami and H. Miyasaka, *Chem. Eur. J.*, 2001, **7**, 3134.

36 D. Gust, T. A. Moore, A. L. Moore, A. N. Macpherson, A. Lopez, J. M. DeGraziano, I. Gouni, E. Bittersmann, G. R. Seely, F. Gao, R. A. Nieman, X. C. Ma, L. J. Demanche, S.-C. Hung, D. K. Luttrull, S.-J. Lee and P. K. Kerrigan, *J. Am. Chem. Soc.*, 1993, **115**, 11141.

37 M. R. Wasielewski, G. L. Gains, III, G. P. Wiederrecht, W. A. Svec and M. P. Niemczyk, *J. Am. Chem. Soc.*, 1993, **115**, 10442.

38 Y.-Z. Hu, S. Tsukiji, S. Shinkai, S. Oishi and I. Hamachi, *J. Am. Chem. Soc.*, 2000, **122**, 241.

39 H. Imahori, D. M. Guldi, K. Tamaki, Y. Yoshida, C. Luo, Y. Sakata and S. Fukuzumi, *J. Am. Chem. Soc.*, 2001, **123**, 6617.

40 D. M. Guldi, H. Imahori, K. Tamaki, Y. Kashiwagi, H. Yamada, Y. Sakata and S. Fukuzumi, *J. Phys. Chem. B*, 2004, **108**, 541.

41 H. Imahori, Y. Sekiguchi, Y. Kashiwagi, T. Sato, Y. Araki, O. Ito, H. Yamada and S. Fukuzumi, *Chem. Eur. J.*, 2004, **10**, in press.

42 Recently a donor (mesityl)–acceptor (acridinium ion) directly linked dyad has been reported to exhibit the longest lifetime of the charge-separated state (2 h at 203 K) with a high quantum yield (98%) in donor–acceptor linked systems. No π conjugation between the donor and acceptor moieties due to the perpendicular orientation may be responsible for formation of the long-lived charge-separated state with the high quantum yield; see: S. Fukuzumi, H. Kotani, K. Ohkubo, S. Ogo, N. V. Tkachenko and H. Lemmetyinen, *J. Am. Chem. Soc.*, 2004, **126**, 1600.

43 N. V. Tkachenko, L. Rantala, A. Y. Tauber, J. Helaja, P. H. Hynninen and H. Lemmetyinen, *J. Am. Chem. Soc.*, 1999, **121**, 9378.

44 K. Tamaki, H. Imahori, Y. Nishimura, I. Yamazaki, A. Shimomura, T. Okada and Y. Sakata, *Chem. Lett.*, 1999, 227.

45 H. Imahori, K. Yamada, M. Hasegawa, S. Taniguchi, T. Okada and Y. Sakata, *Angew. Chem., Int. Ed.*, 1997, **36**, 2626.

46 S. Higashida, H. Imahori, T. Kaneda and Y. Sakata, *Chem. Lett.*, 1998, 605.

47 K. Tamaki, H. Imahori, Y. Nishimura, I. Yamazaki and Y. Sakata, *Chem. Commun.*, 1999, 625.

48 M. Fujitsuka, O. Ito, H. Imahori, K. Yamada, H. Yamada and Y. Sakata, *Chem. Lett.*, 1999, 721.

49 H. Imahori, K. Tamaki, Y. Araki, T. Hasobe, O. Ito, A. Shimomura, S. Kundu, T. Okada, Y. Sakata and S. Fukuzumi, *J. Phys. Chem. A*, 2002, **106**, 2803.

50 A. Helms, D. Heiler and G. McLendon, *J. Am. Chem. Soc.*, 1992, **114**, 6227.

51 (*a*) N. Aratani and A. Osuka, *Bull. Chem. Soc. Jpn.*, 2001, **74**, 1361; (*b*) N. Aratani, A. Osuka, H. S. Cho and D. Kim, *J. Photochem. Photobiol. C*, 2002, **3**, 25; (*c*) D. Kim and A. Osuka, *J. Phys. Chem. A*, 2003, **107**, 8791.

52 H. Imahori, K. Tamaki, Y. Araki, Y. Sekiguchi, O. Ito, Y. Sakata and S. Fukuzumi, *J. Am. Chem. Soc.*, 2002, **124**, 5165.

53 (*a*) T. Hasobe, H. Imahori, H. Yamada, T. Sato and S. Fukuzumi, *Nano Lett.*, 2003, **3**, 409; (*b*) T. Hasobe, H. Imahori, H. Yamada and S. Fukuzumi, *J. Porphyrins Phthalocyanines*, 2003, **7**, 296.

54 (*a*) T. Akiyama, H. Imahori and Y. Sakata, *Chem. Lett.*, 1994, 1447; (*b*) H. Imahori, H. Norieda, S. Ozawa, K. Ushida, H. Yamada, T. Azuma, K. Tamaki and Y. Sakata, *Langmuir*, 1998, **14**, 5335; (*c*) H. Imahori, H. Norieda, Y. Nishimura, I. Yamazaki, K. Higuchi, N. Kato, T. Motohiro, H. Yamada, T. Tamaki, M. Arimura and Y. Sakata, *J. Phys. Chem. B*, 2000, **104**, 1253.

55 (*a*) H. Imahori, T. Azuma, S. Ozawa, H. Yamada, K. Ushida, A. Ajavakom, H. Norieda and Y. Sakata, *Chem. Commun.*, 1999, 557; (*b*) H. Imahori, T. Azuma, A. Ajavakom, H. Norieda, H. Yamada and Y. Sakata, *J. Phys. Chem. B*, 1999, **103**, 7233.

56 (*a*) T. Akiyama, H. Imahori, A. Ajavakom and Y. Sakata, *Chem. Lett.*, 1996, 907; (*b*) H. Yamada, H. Imahori and S. Fukuzumi, *J. Mater. Chem.*, 2002, **12**, 2034.

57 (*a*) D. Hirayama, T. Yamashiro, K. Takimiya, Y. Aso, T. Otsubo, H. Norieda, H. Imahori and Y. Sakata, *Chem. Lett.*, 2000, 570; (*b*) D. Hirayama, K. Takimiya, Y. Aso, T. Otsubo, T. Hasobe, H. Yamada, H. Imahori, S. Fukuzumi and Y. Sakata, *J. Am. Chem. Soc.*, 2002, **124**, 532.

58 (*a*) H. Imahori, H. Yamada, S. Ozawa, K. Ushida and Y. Sakata, *Chem. Commun.*, 1999, 1165; (*b*) H. Imahori, H. Yamada, Y. Nishimura, I. Yamazaki and Y. Sakata, *J. Phys. Chem. B*, 2000, **104**, 2099.

59 S. Fukuzumi and H. Imahori, *Electron Transfer in Chemistry*, ed. V. Balzani, Wiley-VCH, Weinheim, Germany, 2001, Vol. 2, Chapter 8, pp. 927–997.

60 (*a*) H. Imahori, Y. Nishimura, H. Norieda, H. Karita, I. Yamazaki, Y. Sakata and S. Fukuzumi, *Chem. Commun.*, 2000, 661; (*b*) H. Imahori, T. Hasobe, H. Yamada, Y. Nishimura, I. Yamazaki and S. Fukuzumi, *Langmuir*, 2001, **17**, 4925; (*c*) H. Imahori, H. Norieda, H. Yamada, Y. Nishimura, I. Yamazaki, Y. Sakata and S. Fukuzumi, *J. Am. Chem. Soc.*, 2001, **123**, 100.

61 (*a*) H. Yamada, H. Imahori, Y. Nishimura, I. Yamazaki and S. Fukuzumi, *Chem. Commun.*, 2000, 1921; (*b*) H. Yamada, H. Imahori, Y. Nishimura, I. Yamazaki and S. Fukuzumi, *Adv. Mater.*, 2002, **14**, 892; (*c*) H. Yamada, H. Imahori, Y. Nishimura, I. Yamazaki, T. K. Ahn, S. K. Kim, D. Kim and S. Fukuzumi, *J. Am. Chem. Soc.*, 2003, **125**, 9129; (*d*) H. Imahori, K. Hosomizu, Y. Mori, T. Sato, T. K. Ahn, S. K. Kim, D. Kim, Y. Nishimura, I. Yamazaki, H. Ishii, H. Hotta and Y. Matano, *J. Phys. Chem. B*, 2004, **108**, 5018.

62 (*a*) H. Imahori, M. Arimura, T. Hanada, Y. Nishimura, I. Yamazaki, Y. Sakata and S. Fukuzumi, *J. Am. Chem. Soc.*, 2001, **123**, 335; (*b*) S. Fukuzumi, Y. Endo, Y. Kashiwagi, Y. Araki, O. Ito and H. Imahori, *J. Phys. Chem. B*, 2003, **107**, 11979; (*c*) H. Imahori, Y. Kashiwagi, T. Hanada, Y. Endo, Y. Nishimura, I. Yamazaki and S. Fukuzumi, *J. Mater. Chem.*, 2003, **13**, 2890; (*d*) H. Imahori, Y. Kashiwagi, Y. Endo, T. Hanada, Y. Nishimura, I. Yamazaki, Y. Araki, O. Ito and S. Fukuzumi, *Langmuir*, 2004, **20**, 73.

63 (*a*) T. Hasobe, S. Fukuzumi, H. Imahori and P. V. Kamat, *J. Mater. Chem.*, 2003, **13**, 2515; (*b*) T. Hasobe, H. Imahori, S. Fukuzumi and P. V. Kamat, *J. Phys. Chem. B*, 2003, **107**, 12105; (*c*) T. Hasobe, H. Imahori, S. Fukuzumi and P. V. Kamat, *J. Am. Chem. Soc.*, 2003, **125**, 14962; (*d*) T. Hasobe, Y. Kashiwagi, M. Absalom, K. Hosomizu, M. J. Crossley, H. Imahori, P. V. Kamat and S. Fukuzumi, *Adv. Mater.*, 2004, **16**, in press.